(2)

ARMY RESEARCH LABORATORY

A Comparison of In-Bore Projectile Motion From an Electromagnetic Railgun vs. That of a Conventional Cannon Barrel

Lawrence W. Burton

ARL-TR-295 October 1993

NOTICES

REPORT DOCUMENTATION PAGE

Form Approved
OMB No. 0704-0188

1. AGENCY USE ONLY (Leave blank)	2. REPORT DATE	3. REPORT TYPE AND DATES COVERED
	October 1993	Final, Aug 1992 - May 1993

4. TITLE AND SUBTITLE

A Comparison of In-Bore Projectile Motion From an Electromagnetic Railgun vs. That of a Conventional Cannon Barrel

5. FUNDING NUMBERS

PR: 1L162618AH80

6. AUTHOR(S)

Lawrence W. Burton

7. PERFORMING ORGANIZATION NAME(S) AND ADDRESS(ES)

U.S. Army Research Laboratory
ATTN: AMSRL-WT-PD
Aberdeen Proving Ground, MD 21005-5066

8. PERFORMING ORGANIZATION REPORT NUMBER

9. SPONSORING/MONITORING AGENCY NAME(S) AND ADDRESS(ES)

U.S. Army Research Laboratory
ATTN: AMSRL-OP-CI-B (Tech Lib)
Aberdeen Proving Ground, MD 21005-5066

10. SPONSORING/MONITORING AGENCY REPORT NUMBER

ARL-TR-295

11. SUPPLEMENTARY NOTES

12a. DISTRIBUTION/AVAILABILITY STATEMENT

Approved for public release; distribution is unlimited

12b. DISTRIBUTION CODE

13. ABSTRACT *(Maximum 200 words)*

An investigation was undertaken to examine electromagnetic (EM) gun barrel-projectile interaction. The RASCAL code was used in this study because of its ability to easily manipulate relevant parameters such as gun tube centerline, projectile contact stiffness, and projectile design geometry. This work compares the projectile performance in the 9-MJ EM railgun at the University of Texas Center for Electromechanics (UTCEM) to that in a double-travel conventional gun. This comparison was made by varying the parameters listed above for two projectile designs, one projectile being the M829 tank round, the other, a preliminary EM design. It was believed that adoption of this format would identify specific areas of the EM gun-projectile system that excite transverse loading, with the results of this analysis presented here.

14. SUBJECT TERMS

RASCAL, transverse acceleration, EM railgun, in-bore projectile dynamics, velocity, electromagnetic guns

15. NUMBER OF PAGES

34

16. PRICE CODE

17. SECURITY CLASSIFICATION OF REPORT	18. SECURITY CLASSIFICATION OF THIS PAGE	19. SECURITY CLASSIFICATION OF ABSTRACT	20. LIMITATION OF ABSTRACT
UNCLASSIFIED	UNCLASSIFIED	UNCLASSIFIED	SAR

INTENTIONALLY LEFT BLANK.

ACKNOWLEDGEMENT

The author would like to acknowledge Mr. Tom Erline, U.S. Army Research Laboratory, for his assistance and patience in teaching the author how to exercise the RASCAL code. Mr. Erline's insights and experience were drawn upon throughout the course of this analytical investigation. Both he and Dr. Mark Kregel, U.S. Army Research Laboratory, gave many helpful comments during the review of this manuscript.

INTENTIONALLY LEFT BLANK.

TABLE OF CONTENTS

INTENTIONALLY LEFT BLANK.

LIST OF FIGURES

Figure		Page

1. INTRODUCTION

During the past decade, it has been recognized that a projectile's interaction with the gun tube during in-bore travel plays a major role in determining the terminal accuracy of the round. If the projectile is subjected to excessive transverse loading during this period, disturbances may be induced that lead to yawing motion and possibly even excitation of the projectile's natural bending frequencies. Obviously, it is important for the projectile designer to minimize the effects of these interactions.

In recent years, much effort has been devoted to developing modeling techniques that may be used to estimate the disturbances that arise from projectile-gun tube interaction. These models range in scope from a one-dimensional (1-D) beam element code, RASCAL (Erline, Kregel, and Pantano 1990), to commercial three-dimensional (3-D), transient analysis finite element programs. The use of these techniques to investigate gun-projectile dynamics in conventional tank cannons is well documented (Erline and Kregel 1990; Hopkins 1990; Manners 1990; Polcyn and Cox 1990; Rabern and Bannister 1990; Wilkerson 1993).

Currently, there are ongoing programs to develop alternatives to conventional powder guns. One example is the electromagnetic (EM) gun system, which relies on passing current through an armature in an induced magnetic field to provide its propulsive force. The EM gun barrels are composite in nature since they require both insulators and rails in their construction and have a non-homogeneous cross section (see Figure 1). This is a radical departure from the cylindrical steel tubes characteristic of conventional cannons. In addition, solid armature railguns typically rely on metal-to-metal contact to conduct current between the gun rails and the armature which leads one to believe the EM system has characteristics that may lead to more excessive transverse disturbances being imparted to the projectile.

An analysis was undertaken to determine the severity of transverse loading in an EM barrel in comparison to a conventional steel gun tube. This report details the analytical investigation and presents the results

2. PURPOSE

The purpose of this analytical investigation was to determine the severity of transverse loading in an EM barrel in comparison to a conventional steel gun tube. It was conjectured that by running

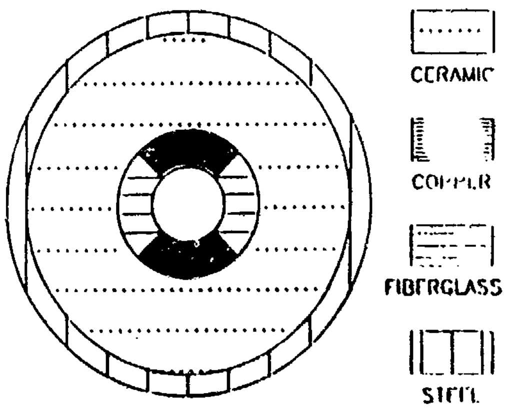

Figure 1. EM railgun barrel cross section.

numerous case studies while varying some of the parameters that affect a projectile's in-bore motion, a cause-and-effect relationship could be identified by isolating the conditions that produce the various projectile responses.

3. PROCEDURE

Realizing the gross difference between conventional and EM gun systems, it was advantageous to exercise a simplistic in-bore dynamics code, which would allow for easy manipulation of the relevant parameters. This led to selection of the RASCAL code as the vehicle for conducting the investigation. RASCAL is a 1-D code which employs beam elements and requires inputs of interior ballistic loading information, projectile geometry, barrel dimensions, and centerline profile, as well as breech and gun system parameters. The specific values incorporated into the model are detailed in the following sections.

4. GUN BARREL MODELING

The study focused on a comparison of projectile motion in an EM railgun with that of a conventional double-travel gun. The 9-MJ railgun at the University of Texas Center for Electromechanics (UTCEM) was selected as the railgun to be modeled because centerline measurements for the barrel exist. The existence of centerline data is noteworthy. The EM community has only recently begun to recognize the important role the centerline profile plays in determining in-bore motion. It is important to note that the centerline profile changes drastically from shot to shot even with current state-of-the-art railgun systems.

Railguns are typically honed out after every shot to eliminate the damage done by current arcing between the armature and the rails, as well as by wear, thus placing the in-bore geometry in a continual state of fluctuation. Therefore, the data employed in the RASCAL code are a one-time barrel centerline meant to be representative of those that typically occur in the UTCEM gun.

The UTCEM gun is 9.5 m long. It is mounted vertically to eliminate the need to consider tube droop because of gravity. Correspondly, the RASCAL runs for the EM centerline profile cases were all made assuming no effects due to gravity. Also, the UTCEM barrel has a constant diameter cylindrical cross section along its entire length. A double-travel conventional gun was chosen to serve as a comparator because its 10-m length is nearly equivalent to that of the UTCEM barrel and allows for velocities above those of standard ordnance, which approach those predicted for the railgun. A schematic of the gun barrel geometries is depicted below in Figure 2.

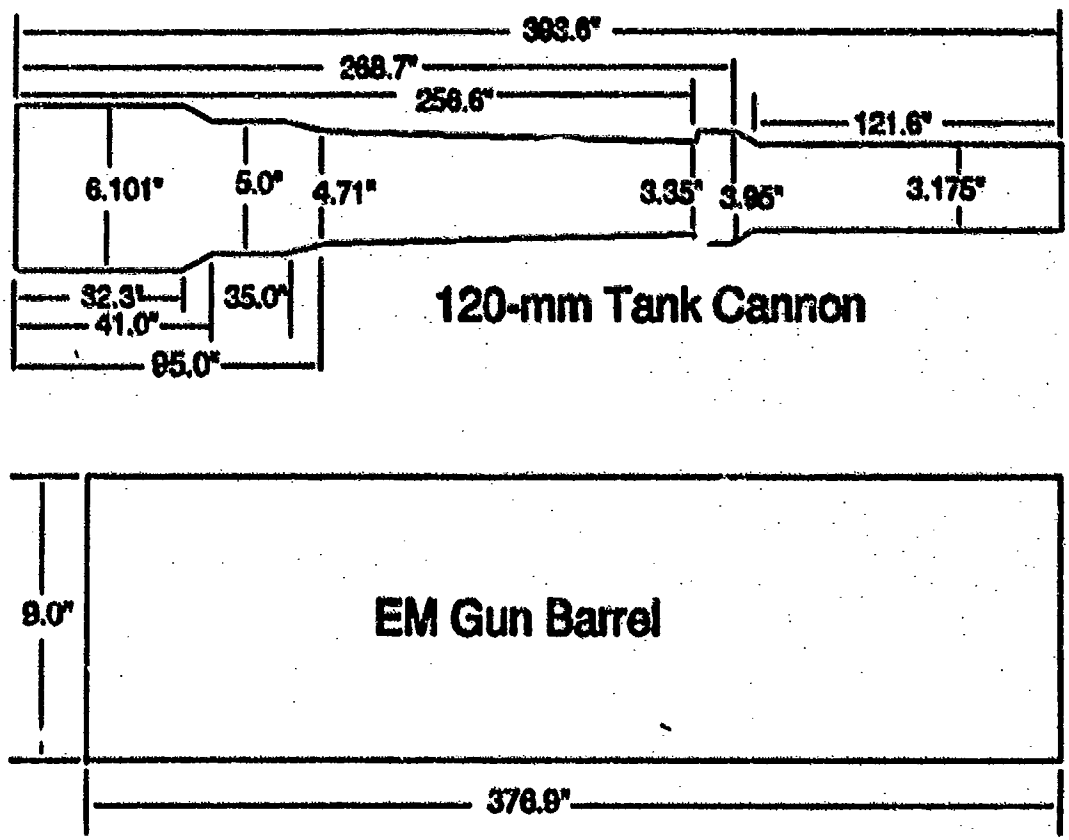

Figure 2. Barrel geometries of EM and double-travel guns.

The two barrels modeled have different bore diameters: the EM railgun has a 90-mm nominal diameter, while the double-travel cannon is 120 mm. One of the benefits of RASCAL is it does not require barrel geometry to be consistent with projectile geometry. Thus, it is possible to examine the motion of a 120-mm projectile in a 90-mm bore and vice versa. This capability results from RASCAL's use of beam elements to model the projectile, and the projectile contact points represented with springs which interact with the gun model's beam elements.

Figure 3 shows the centerline data incorporated into the gun barrel models. For the EM railgun, the vertical measurements are defined by the copper rails, while the horizontal are for the ceramic insulators. The solid line of tube 008 data refers to a double-travel cannon, and data line 2 is simply a verification of the original measurements of the UTCEM gun shown as data line 1.

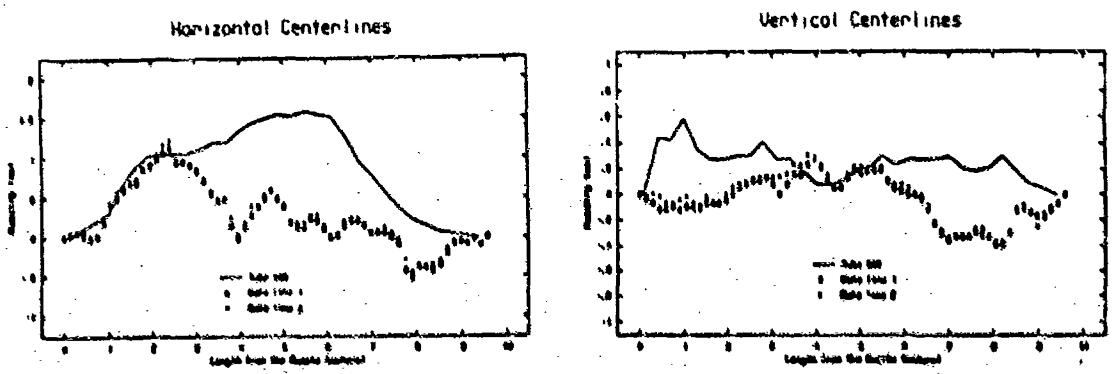

Figure 3. Gun barrel centerline measurements.

The final input requirement pertaining to the barrels was descriptions of the breech and gun system parameters. Since both guns are experimental (i.e., not meant for vehicle mounting), it was decided to use identical input files for the two guns except for bore and chamber radii particular to each gun, as well as the elastic modulus and material density of the barrels.

Obviously, for the case of the homogeneous steel conventional gun, the modulus (30e06 lb/in^2) and density (0.283 lb/in^3) are known. The EM barrel is not as straightforward, and the laminate nature of its cross section calls for derivation of an effective modulus and density. An effective density was calculated using a simple rule of mixtures approach, whereby the density of each material layer was multiplied by its volume, and these values were summed to give the total barrel weight. This weight was then divided by the total volume to provide an effective density of the barrel (0.193 lb/in^3). A similar method was used

to derive an effective modulus using a beam-deflection analysis. If each layer is considered a beam that maintains contact with its adjacent layer, the deflections are equivalent at coincidental points and have values of the form $y = (wl^4)/(8EI)$. This leads to

$$Y_1 = Y_2 = Y_3 = \frac{w_1 l^4}{8E_1 I_1} = \frac{w_2 l^4}{8E_2 I_2} = \frac{w_3 l^4}{8E_3 I_3} = Y_{eff} = \frac{w_{eff} l^4}{8E_{eff} I_{eff}}$$

in which the subscripts denote the different layers. Since the barrel hangs vertically, there is no distributed gravity load, so $w_1 = w_2 = w_3 = w_{eff}$ for any transverse distributed load. This results in

$$E_{eff}I_{eff} = E_1I_1 + E_2I_2 + E_3I_3$$

The resultant effective modulus calculated equals 35.7e06 lb/in^2.

5. INTERIOR BALLISTIC MODELING

One of the most significant differences between the EM railgun and the conventional gun system is the means of providing the propulsive force. However, the RASCAL code allows for interior ballistic data to be input as velocity vs. time and is thus transparent to the mode of propulsion.

Two separate interior ballistic curves were used in the analysis and are shown in Figure 4. The first curve (and the more severe case) shows a peak velocity of 1,965 m/s at muzzle exit. This curve was provided by UTCEM from a simulation code developed in-house. It is important to realize this simulation does not accurately reflect the current status of the UTCEM gun system for large caliber projectiles. At present, rise times of about 100 μs are typical, with efforts ongoing to control the staging of generators to reduce the rise time to that shown in the simulation. Therefore, this curve represents an optimal interior ballistic loading from the EM railgun.

The second load profile is for an M829 projectile fired from a double-travel cannon and does not include any charge optimization. This case achieves a maximum velocity of 1,743 m/s at exit.

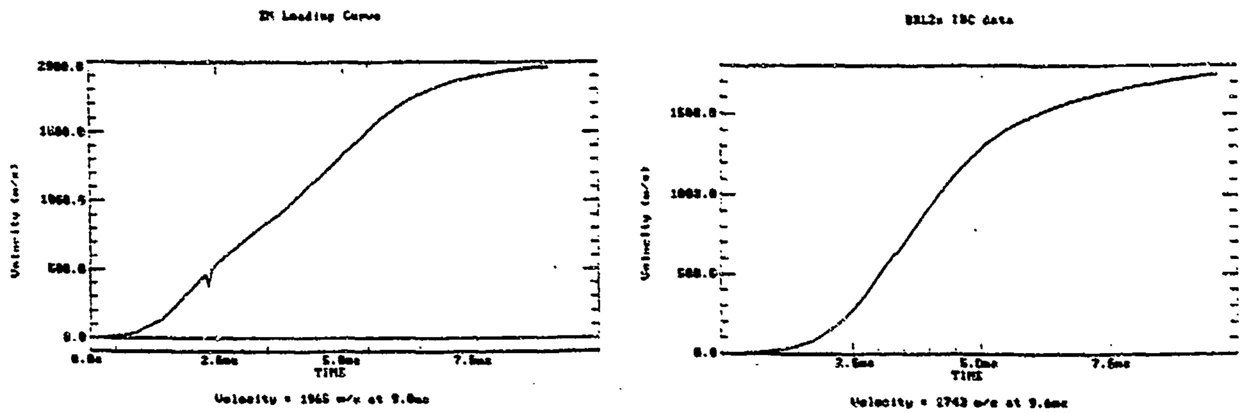

Figure 4. Interior ballistic curves used in RASCAL analysis.

6. PROJECTILE GEOMETRY

RASCAL was written for specific application to projectiles operating in conventional tank cannons. Some of the assumptions required to apply the code to the EM railgun cases have been detailed previously in the gun barrel modeling section. Similarly, a set of assumptions was required in modeling the EM projectile with RASCAL.

Two generic geometries are available within RASCAL for modeling projectiles. They are a double-ramp configuration as occurs in the M829 and the geometry of a HEAT round. The EM projectile of interest is shown in Figure 5 and has the basic double-ramp configuration with two trailing armature contacts attached. Modeling these two trailing arms presents a difficulty since RASCALs input is in the form of various tapers and a forward borerider as shown in Figure 6.

Figure 5. EM projectile configuration.

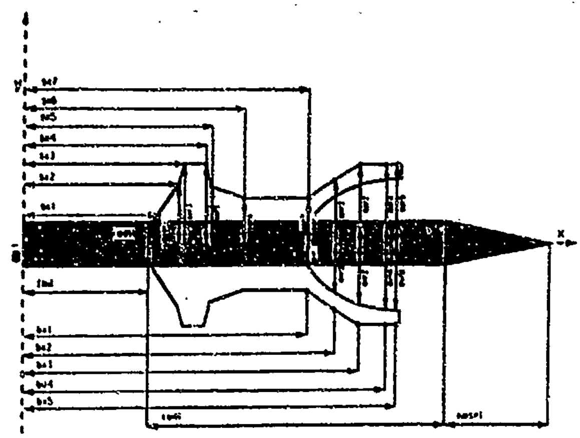

Figure 6. RASCAL input geometry for a double-ramp sabot.

The RASCAL model of the EM projectile is depicted in Figure 7. The swept-back portion of the chevron armature design is not included because of the limitations of the RASCAL geometry modeler. However, it was felt that the overhanging structure provides only minimal additional lateral stiffness, so that the model would yield a response fairly representative of the projectile.

Some preliminary calculations were also made to investigate the possibility of reversing the projectile direction to model one of the armature leaves by taking advantage of the forward borerider modeling capability (see Figure 8). From these calculations, it was found that the placement of the contact point greatly affected the response of the projectile because of the way RASCAL resolves the boreriding structure into beam elements. Therefore, the representation shown in Figure 7 served as the EM projectile model used throughout the analysis.

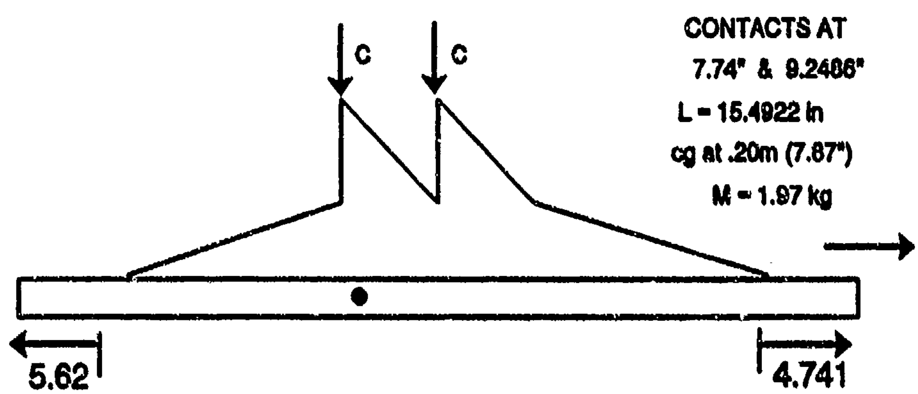

Figure 7. RASCAL model of EM projectile.

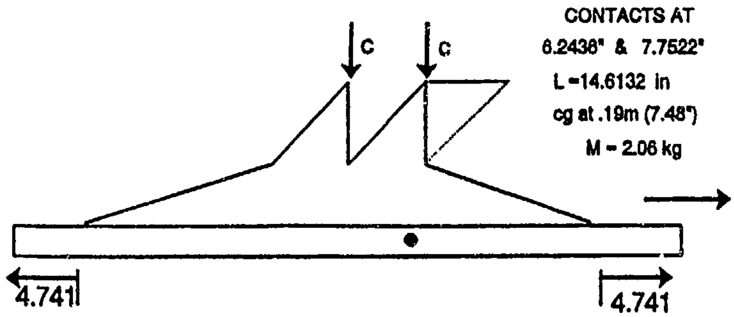

Figure 8. Alternate model of the EM projectile.

The other projectile incorporated in the study was the M829, which is a standard ammunition for the 120-mm cannon. This was meant to serve as a baseline performer against which the EM design could be evaluated.

A key parameter in determining a projectile's in-bore performance is the stiffness associated with the projectile/bore interface. Attempts have been made to experimentally determine this contact stiffness value (Lyon 1993; McCall and Henry, to be published) with results ranging from approximately 1.0e05 to 1.0e06 lb/in in magnitude. Previous experience in matching the RASCAL output results with test firing data led to the use of 4.3e05 lb/in as a standard value (Erline 1991). For the purpose of this investigation, three contact stiffness values were evaluated for each case studied to represent the lowest measured value (1.0e05 lb/in), the highest measured value (1.0e06 lb/in), and a value used in previous evaluations with RASCAL (4.3e05 lb/in).

7. CASE STUDY MATRIX

The analysis involved the two projectile models with system parameters varied to look at 11 different scenarios as listed in Table 1. Each of the 11 cases were run with the three stiffness values resulting in 33 individual cases being investigated.

The study was set up so that Cases 1 and 2 represented an estimate of the M829 projectile response from the double-travel gun having a conventional pressure profile loading with the measured horizontal and vertical centerlines, respectively. Case 3 was run to see what effect the more severe EM loading profile would have on the projectile. Case 4 isolated the effects attributable to the rail centerline, while Cases 5 and 6 provided data for the M829 projectile in the EM gun system while traversing the rail and insulator centerlines, respectively.

Table 1. Listing of Parameters for Each Case Investigated

	Projectile	Loading	Centerline	Gun System	Barrel Geometry
Case 1	M829	Conventional	Double Travel 120 mm	Double Travel Cannon	Double Travel Cannon
Case 2	M829	Conventional	Double Travel 120 mm (vertical)	Double Travel Cannon	Double Travel Cannon
Case 3	M829	EM Profile	Double Travel 120 mm	Double Travel Cannon	Double Travel Cannon
Case 4	M829	Conventional	UTCEM Rails	Double Travel Cannon	Double Travel Cannon
Case 5	M829	EM Profile	UTCEM Rails	UTCEM	UTCEM
Case 6	M829	EM Profile	UTCEM Insulator	UTCEM	UTCEM
Case 7	EM	EM Profile	UTCEM Insulator	UTCEM	UTCEM
Case 8	EM	EM Profile	UTCEM Rails	UTCEM	UTCEM
Case 9	EM	Conventional	UTCEM Rails	UTECM	UTCEM
Case 10	EM	EM Profile	Double Travel 120 mm	UTCEM	UTCEM
Case 11	EM	Conventional	Double Travel 120 mm (vertical)	Double Travel Cannon	Double Travel Cannon

The other half of the investigation focused on the response of the EM projectile, with Case 7 serving as a baseline for the complete EM system with the centerline being that measured for the insulators. Likewise, Case 8 was set up similar to that of Case 7 but used the centerline profile of the rails. As with the M829 projectile cases, parameters were shuffled to see how singular changes affected in-bore performance. Case 9 subjected the EM projectile design to the conventional loading but in the EM gun system. Case 10 examined the projectile's actions in an EM system having the double-travel gun's centerline. Finally, Case 11 analyzed the EM projectile in the conventional gun system.

8. RESULTS

The output available from RASCAL includes a wealth of information to determine both projectile and gun response. The focus of this effort was on the in-bore response of the round so the information extracted and examined from the RASCAL output for each case studied included the transverse velocity at the projectile center of gravity and the projectile angular velocity over the length of in-bore travel.

The transverse acceleration of each projectile's center of gravity was determined by taking a derivative of the calculated RASCAL velocity with a subsequent conversion made into g's. These values are tabulated in Table 2 for the 11 cases examined for all three contact stiffness values. Figure 9 is a graphical display of the same information. While the EM projectile cases generally exhibit higher transverse accelerations, they, for the most part, are of the same order of magnitude as the M829 cases. The disturbing fact of these results is the dramatic rise in lateral acceleration for both projectiles traveling through the EM gun with the insulator centerline (Cases 6 and 7). The M829 cases exhibit increasing accelerations as the contact stiffness is increased. This is to be expected since the projectile's center of gravity is beneath the rear contact so that any increase in force transmitted through the stiffer contact acts directly upon the center of gravity. Conversely, the EM projectile has its center of gravity between the two contact points. The data reveal the medium stiffness value (4.3e05 lb/in) results in a more aggravated transverse acceleration than the stiffest contact (1.0e06 lb/in). This may be because one of the rod's natural bending frequencies is excited when the medium stiffness is assumed.

Table 2. Maximum Transverse Accelerations

Maximum Transverse Acceleration, g's							
k, lb/in	1.0e05	4.3e05	1.0e06	k, lb/in	1.0e05	4.3e05	1.0e06
Case 1	534	649	1,492	Case 7	2,227	5,973	4,321
Case 2	211	594	673	Case 8	1,882	3,152	2,142
Case 3	552	857	1,615	Case 9	1,722	3,215	1,941
Case 4	247	845	2,406	Case 10	1,442	1,563	2,139
Case 5	296	1,249	2,585	Case 11	1,185	1,517	1,122
Case 6	884	1,868	8,498				

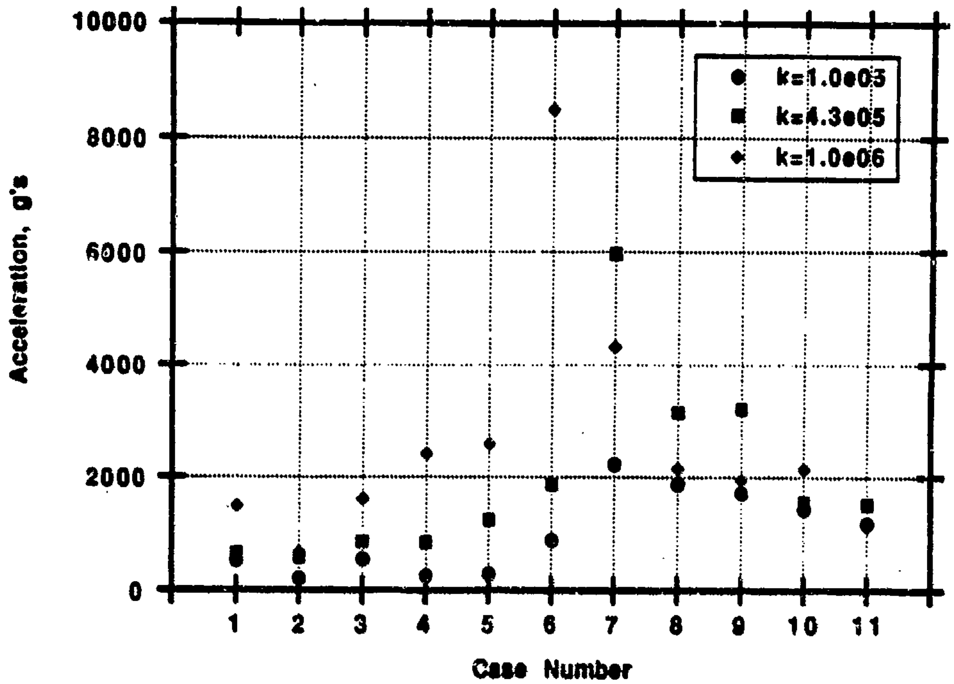

Figure 9. Comparison of transverse accelerations.

It is also interesting to notice the trends in the magnitude of the transverse acceleration values. Proceeding from left to right on Figure 9, Cases 1 through 6 show increasing peak lateral accelerations. This corresponds to the M829 being subjected to more "EM-like conditions" with each subsequent case. That is, Cases 1 and 2 employ conventional gun system parameters, Cases 3 and 4 have some aspects of the EM system integrated into them, and Cases 5 and 6 have the M829 in the full EM environment.

Similarly, Cases 7 to 11 show that as the EM projectile is introduced to more elements of the conventional gun system (again, moving left to right), it alleviates the severity of the transverse acceleration. Case 7 with the insulator profile serves as a stark contrast to Case 11, the conventional gun system parameter case, clearly pointing out the differences between the conventional and EM gun systems.

The other output examined from the RASCAL analysis was the data for the angular rate of the projectile. These data are a measure of the instantaneous velocity of the projectile model slope, based on the displacement of the contact points. This provides a feel for the magnitude of a projectile's yawing motion while in bore. Plots of the angular velocity vs. time are presented in Figures 10 through 42 for the 11 case studies with the various contact stiffness values.

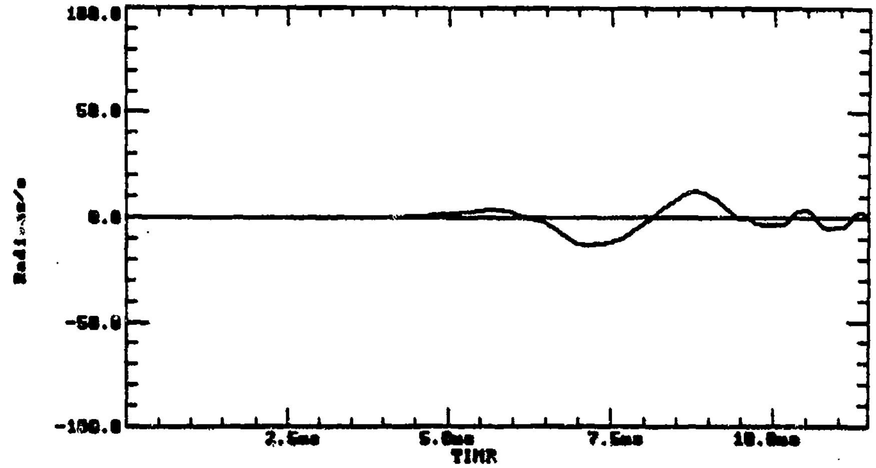

Figure 10. Angular velocity of case 1, k=1.0e05 lb/in.

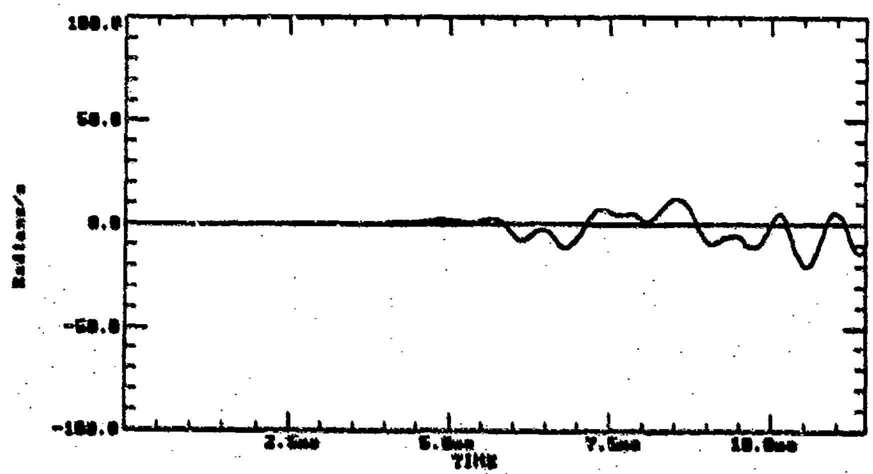

Figure 11. Angular velocity of case 1, k=4.3e05 lb/in.

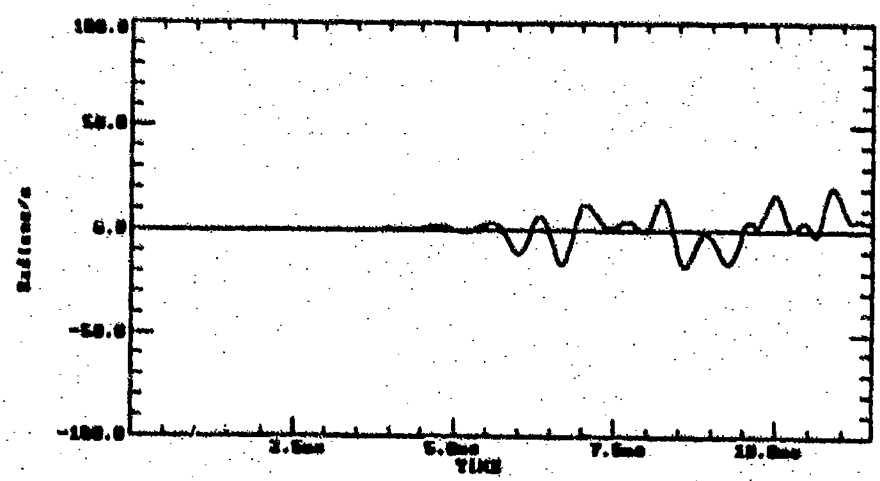

Figure 12. Angular velocity of case 1, k=1.0e06 lb/in.

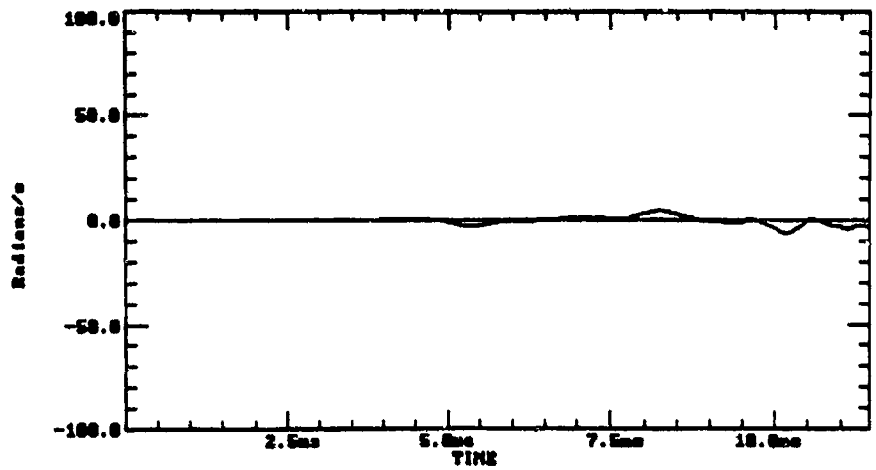

Figure 13. Angular velocity of case 2, k=1.0e05 lb/in.

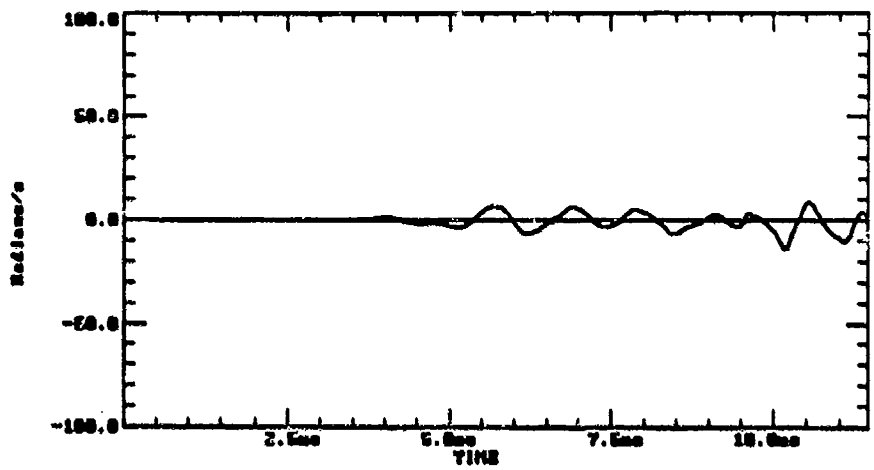

Figure 14. Angular velocity of case 2, k=4.3e05 lb/in.

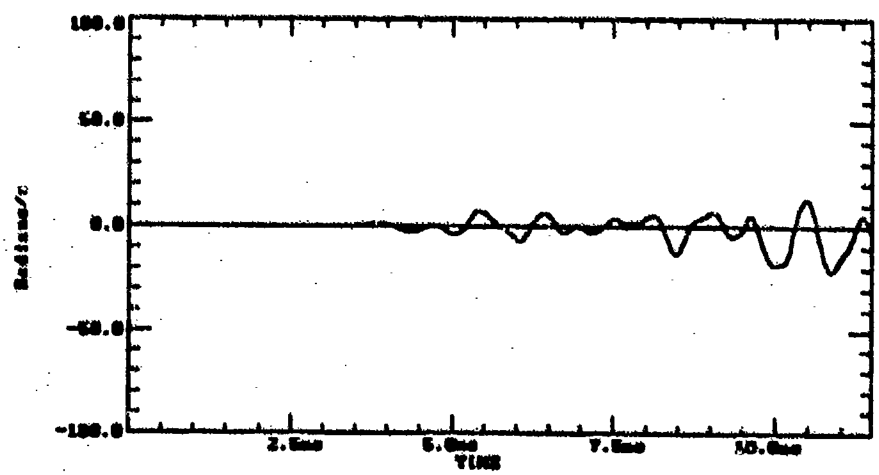

Figure 15. Angular velocity of case 2, k=1.0e06 lb/in.

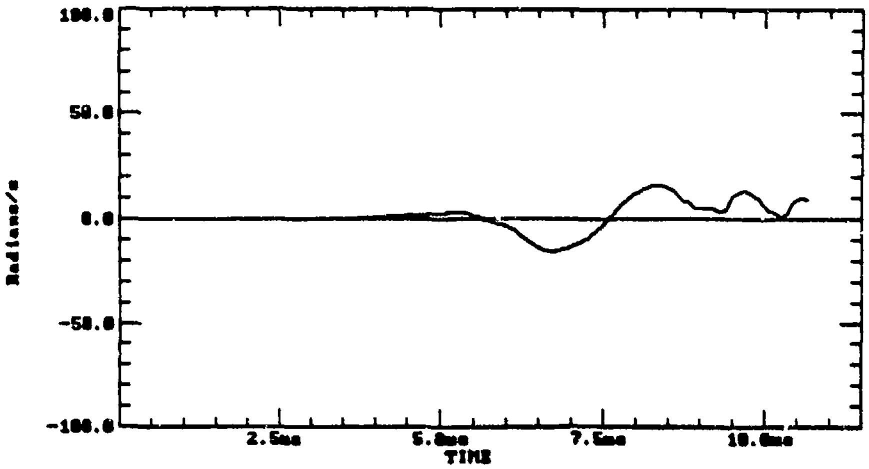

Figure 16. Angular velocity of case 3, k=1.0e05 lb/in.

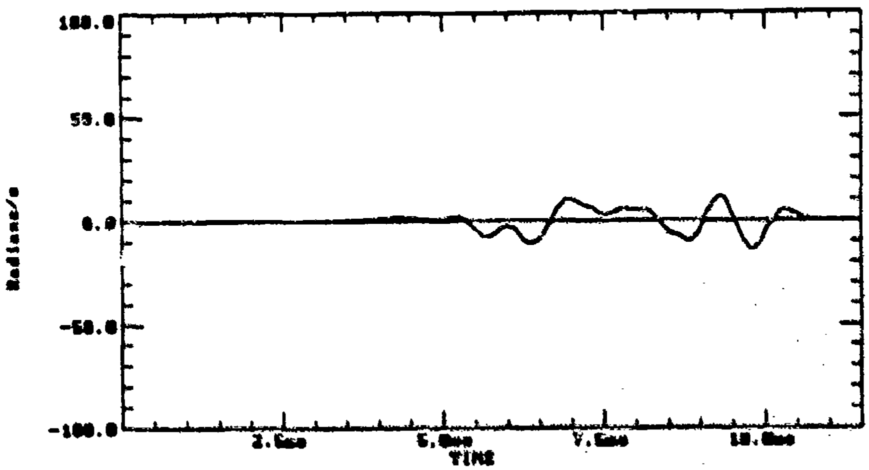

Figure 17. Angular velocity of case 3, k=4.3e05 lb/in.

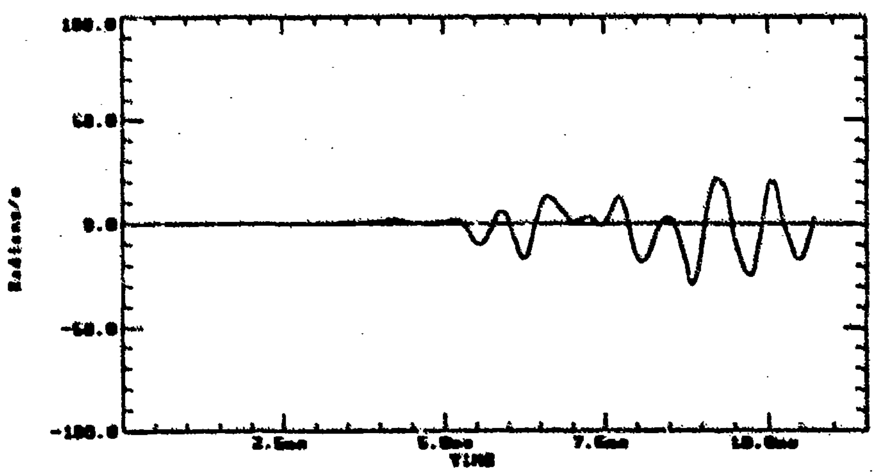

Figure 18. Angular velocity of case 3, k=1.0e06 lb/in.

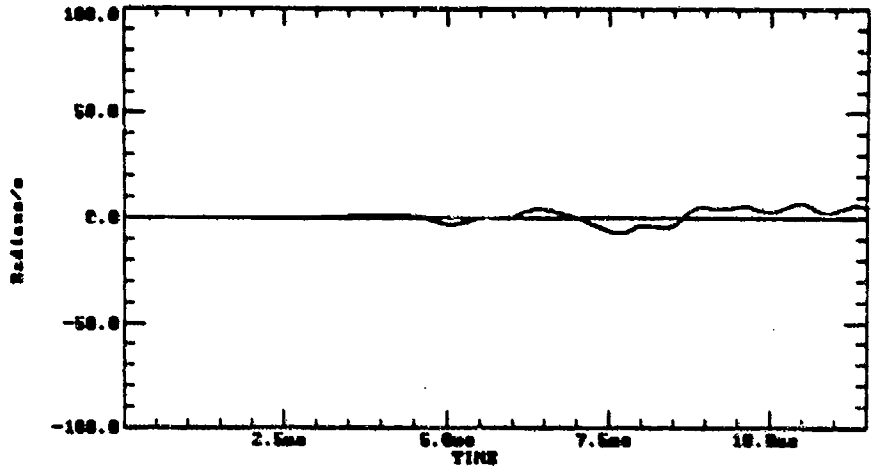

Figure 19. Angular velocity of case 4, k=1.0e05 lb/in.

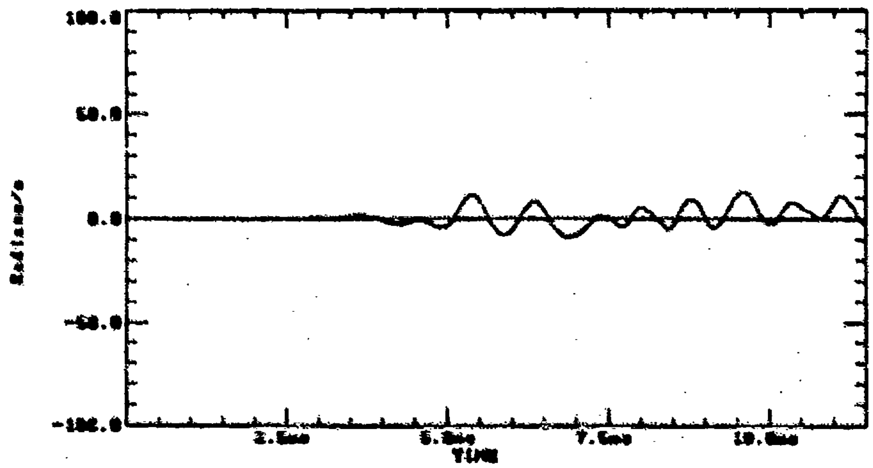

Figure 20. Angular velocity of case 4, k=4.3e05 lb/in.

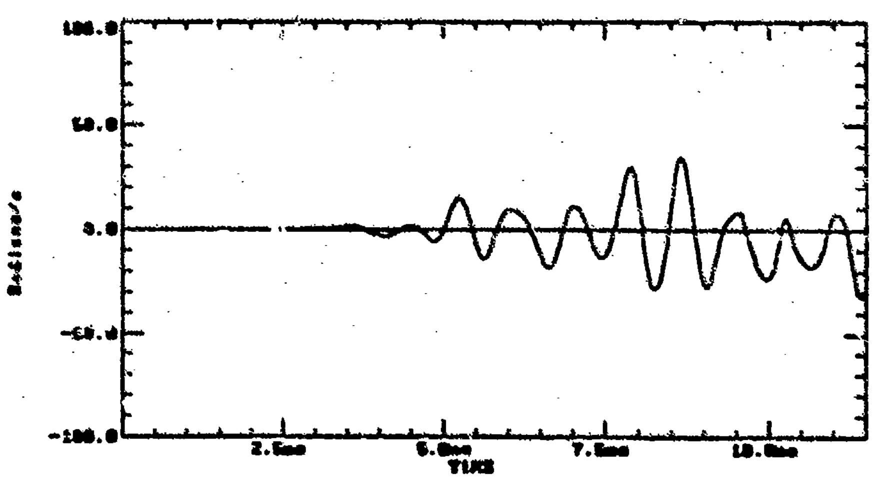

Figure 21. Angular velocity of case 4, k=1.0e06 lb/in.

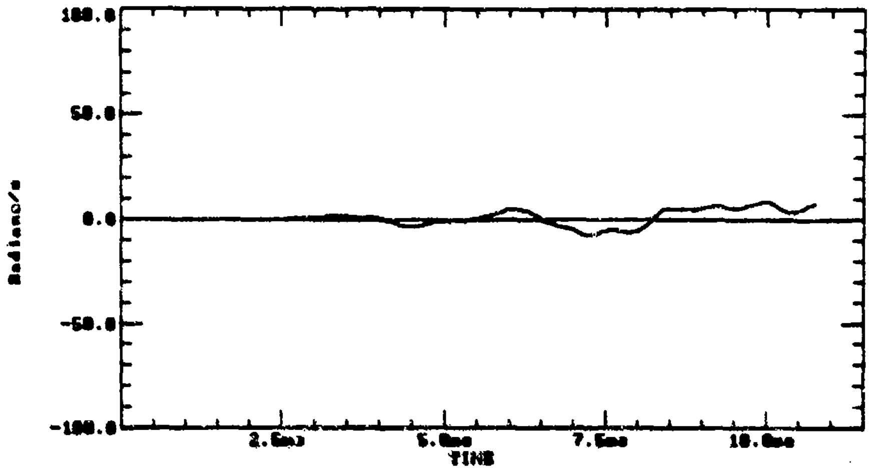

Figure 22. Angular velocity of case 5, k=1.0e05 lb/in.

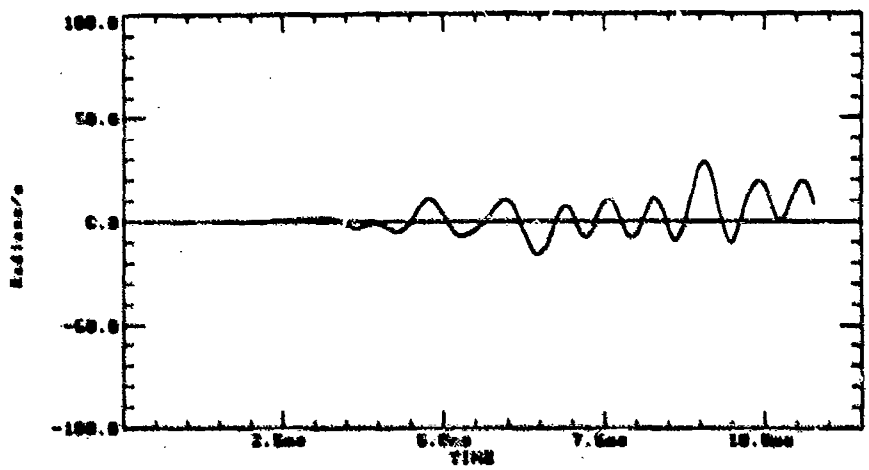

Figure 23. Angular velocity of case 5, k=4.3e05 lb/in.

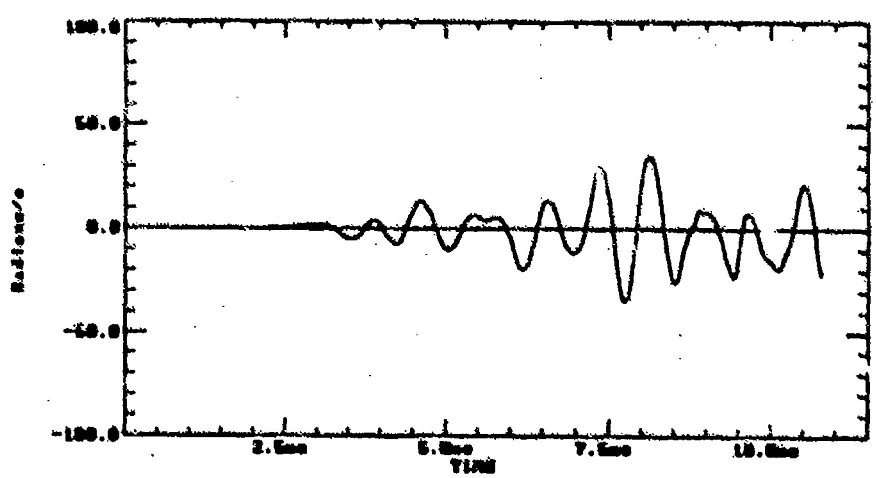

Figure 24. Angular velocity of case 5, k=1.0e06 lb/in.

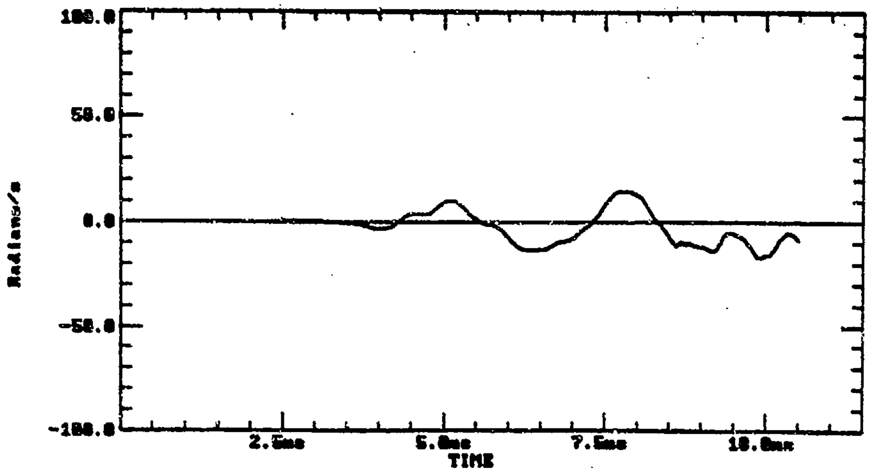

Figure 25. Angular velocity of case 6, k=1.0e05 lb/in.

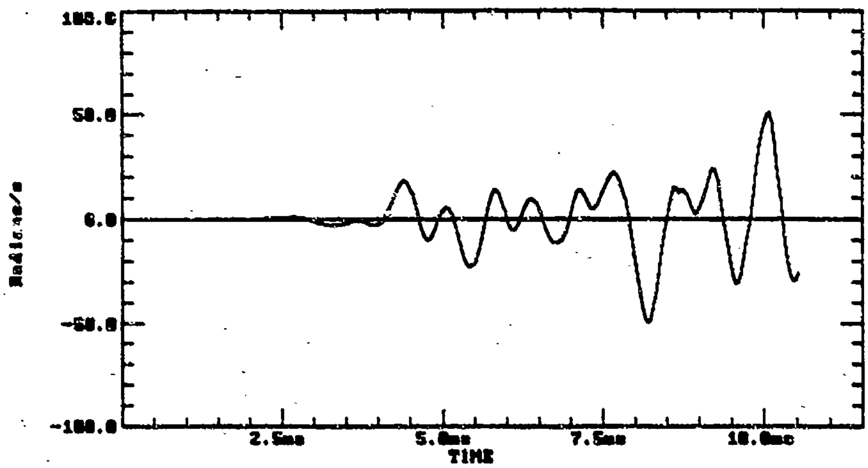

Figure 26. Angular velocity of case 6, k=4.3e05 lb/in.

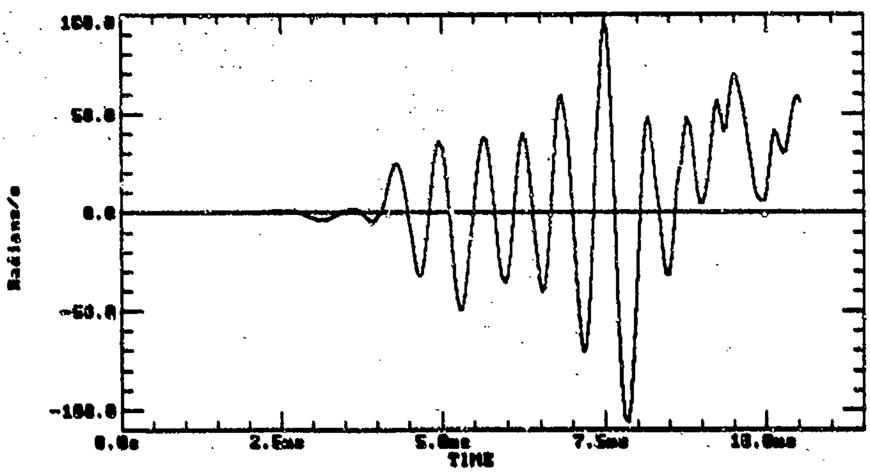

Figure 27. Angular velocity of case 6, k=1.0e06 lb/in.

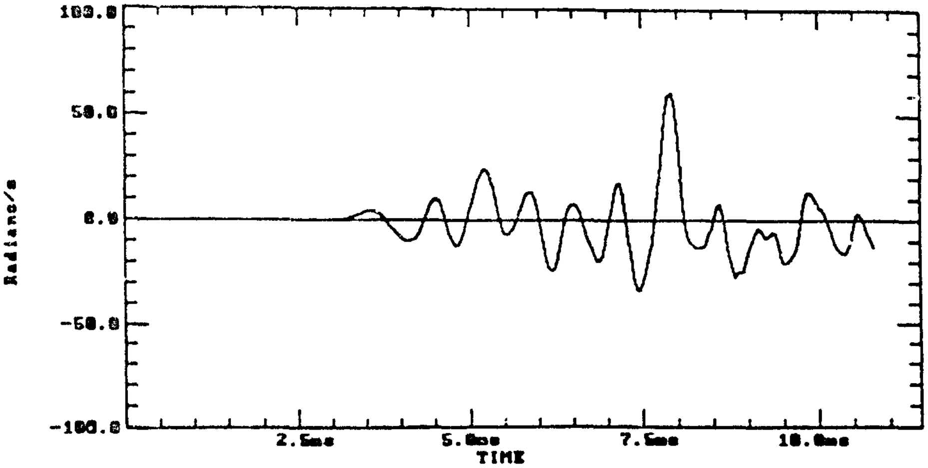

Figure 28. Angular velocity of case 7, k=1.0e05 lb/in.

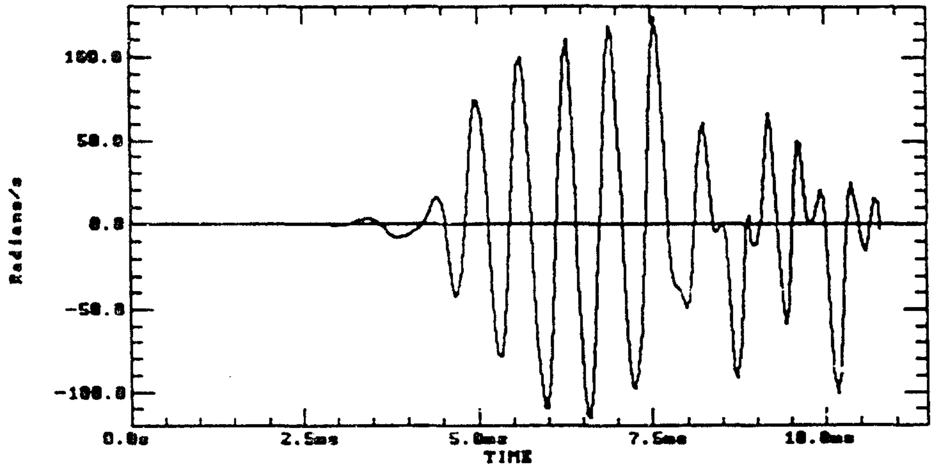

Figure 29. Angular velocity of case 7, k=4.3e05 lb/in.

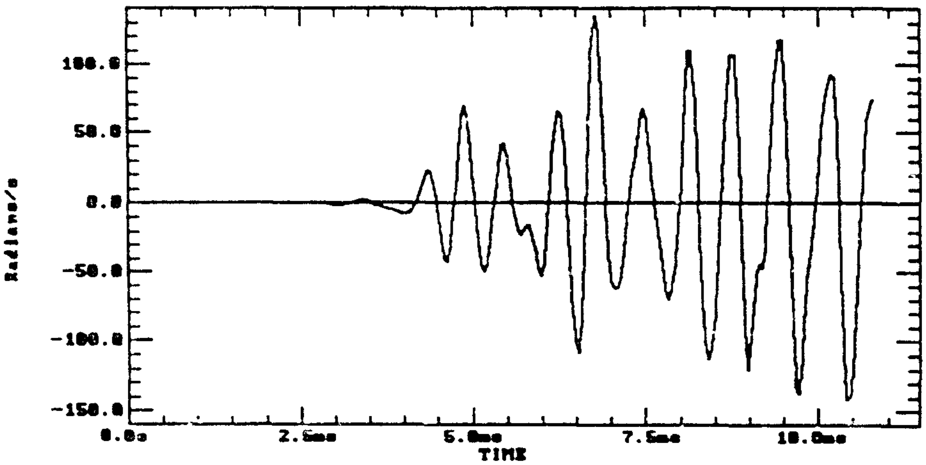

Figure 30. Angular velocity of case 7, k=1.0e06 lb/in.

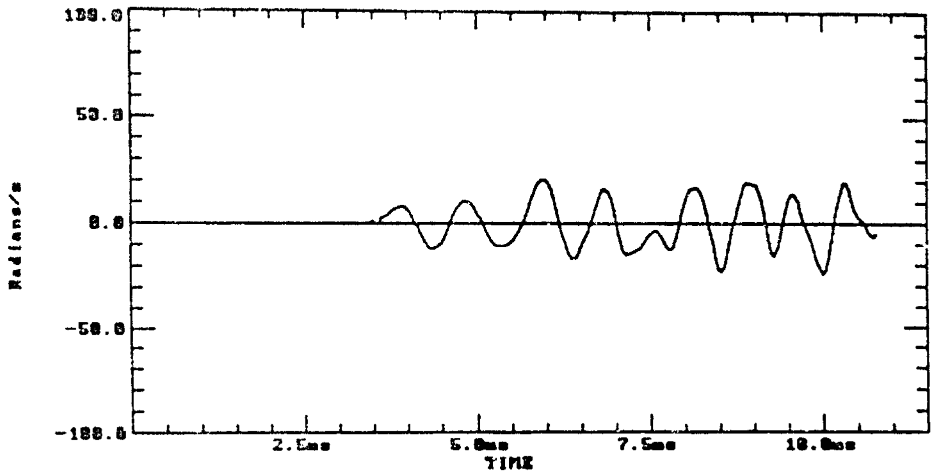

Figure 31. Angular velocity of case 8, k=1.0e05 lb/in.

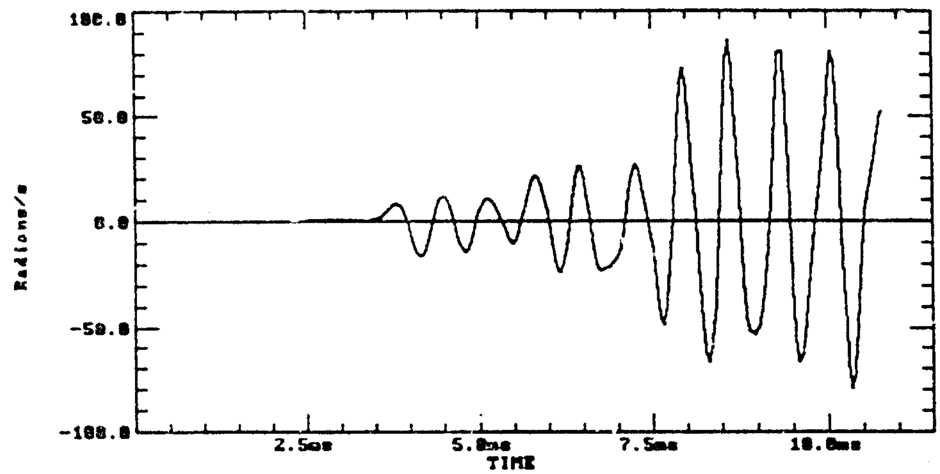

Figure 32. Angular velocity of case 8, k=4.3e05 lb/in.

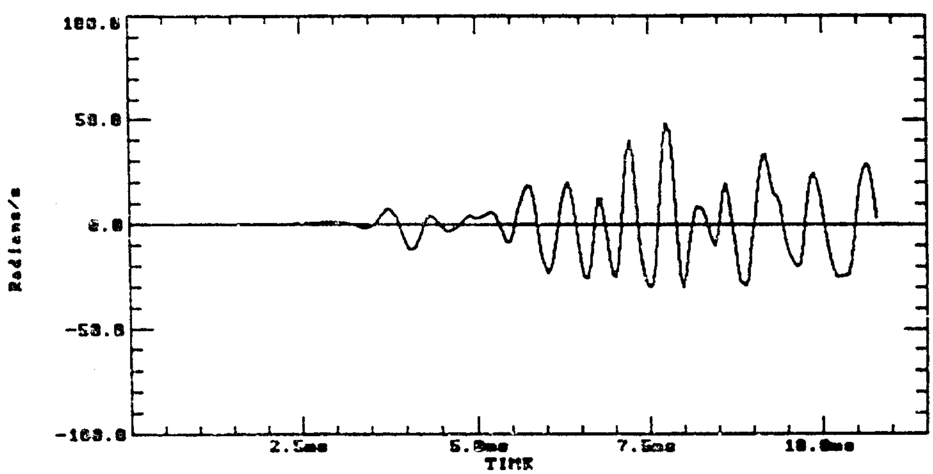

Figure 33. Angular velocity of case 8, k=1.0e06 lb/in.

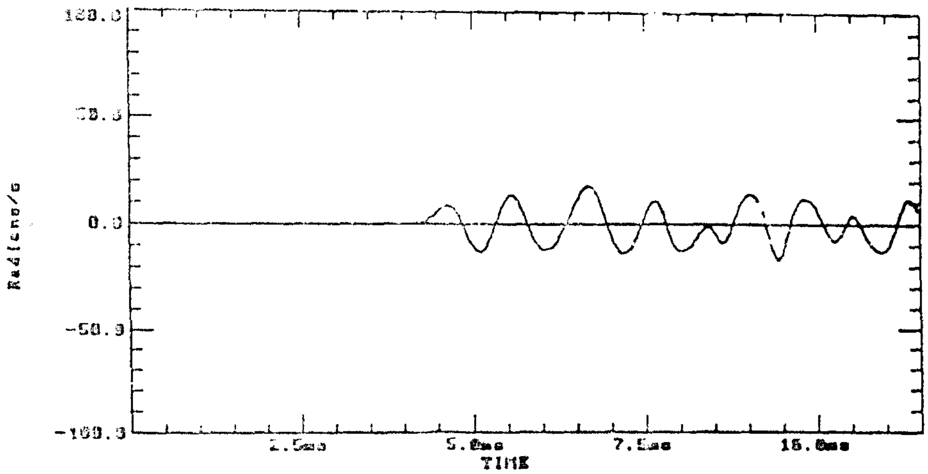

Figure 34. Angular velocity of case 9, k=1.0e05 lb/in.

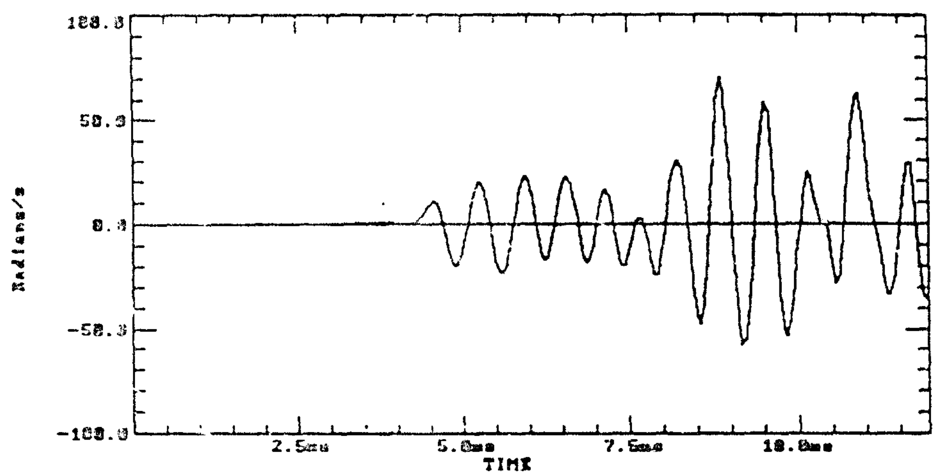

Figure 35. Angular velocity of case 9, k=4.3e05 lb/in.

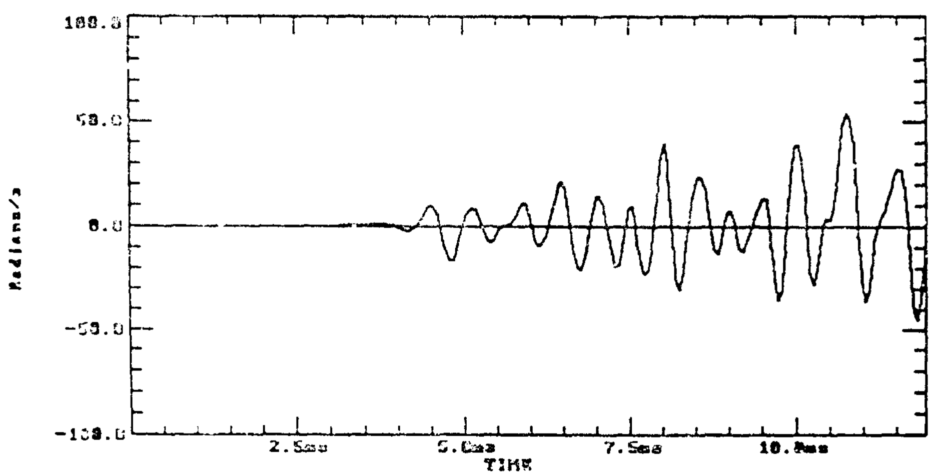

Figure 36. Angular velocity of case 9, k=1.0e06 lb/in.

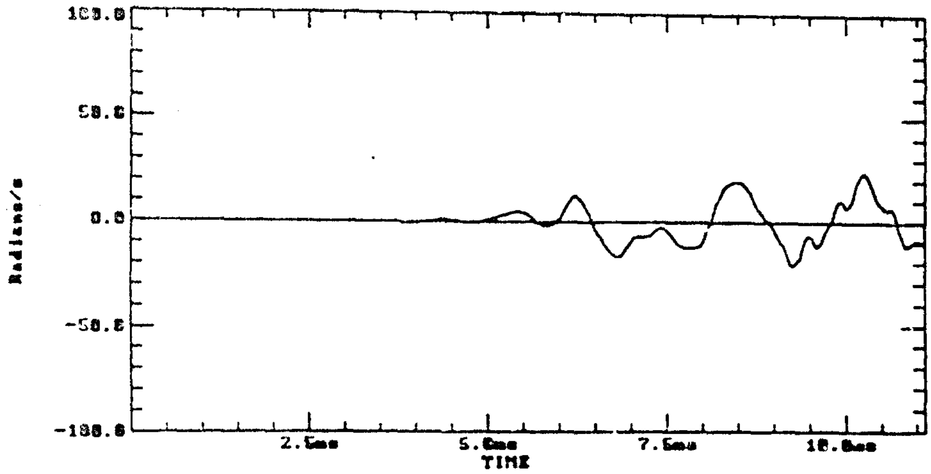

Figure 37. Angular velocity of case 10, k=1.0e05 lb/in.

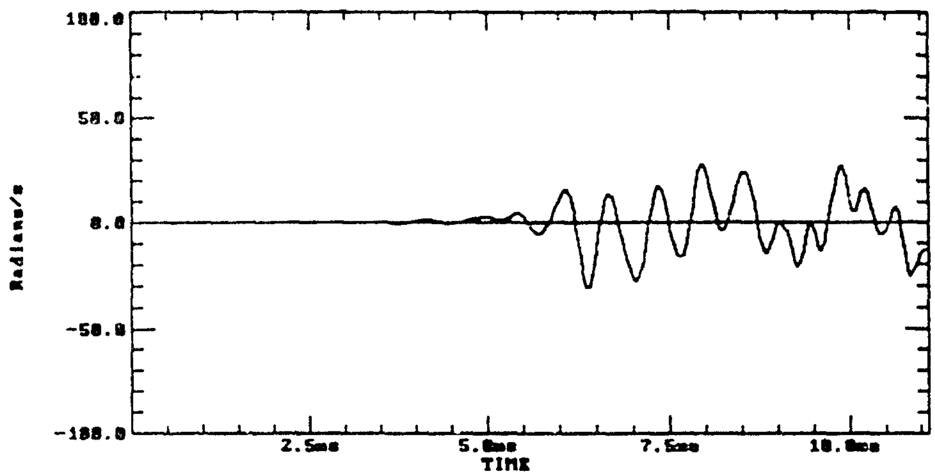

Figure 38. Angular velocity of case 10, k=4.3e05 lb/in.

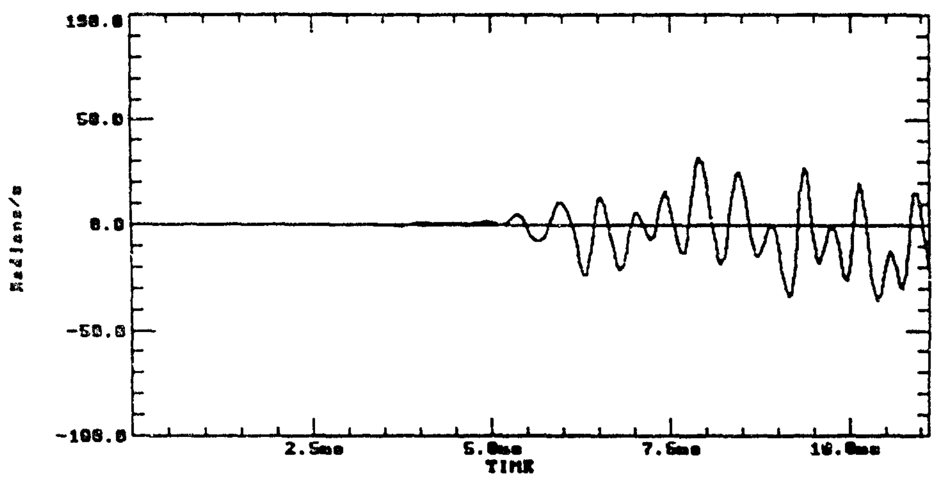

Figure 39. Angular velocity of case 10, k=1.0e06 lb/in.

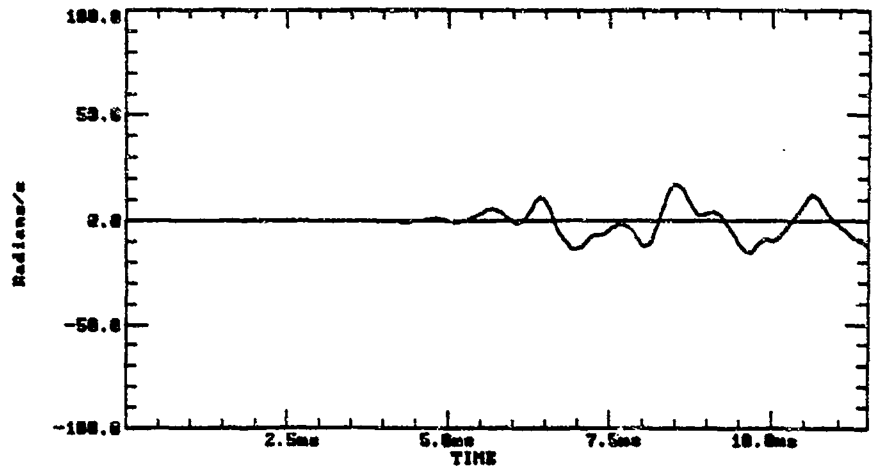

Figure 40. Angular velocity of case 11, k=1.0e05 lb/in.

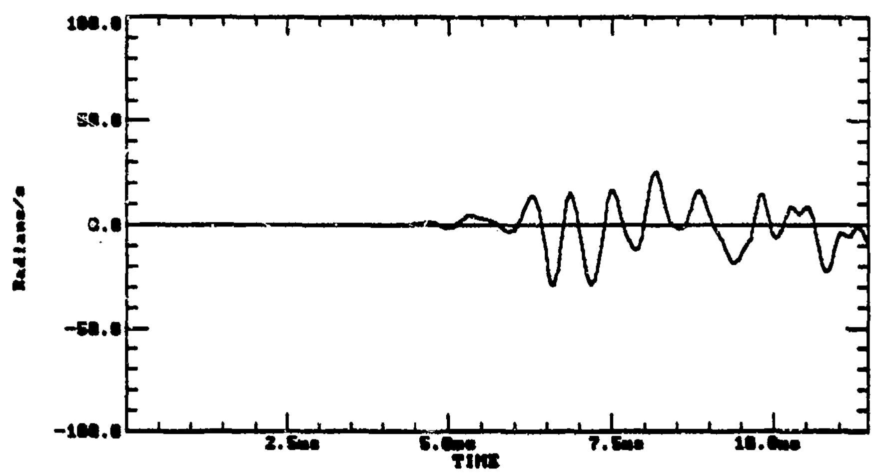

Figure 41. Angular velocity of case 11, k=4.3e05 lb/in.

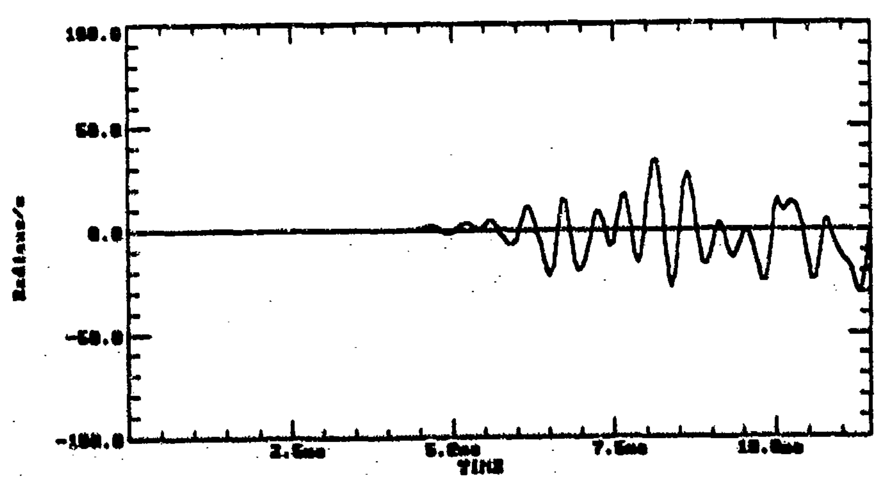

Figure 42. Angular velocity of case 11, k=1.0e06 lb/in.

From the plots, it is seen that the M829 with soft contacts (k=1.0e05 lb/in) yields a rather benign response for all cases (Cases 1–6). By comparing Cases 1 and 4 with Cases 3 and 5, respectively, one finds the projectile motion is mostly unaffected by a change in load profile for this velocity regime. Substitution of the rail centerline profile for the conventional double travel (Case 1 vs. Case 4 and Case 3 vs. Case 5) reveals a slight exacerbation of the in-bore motion. In general, the yawing motion worsens with an increase in contact stiffness. The case of the M829 through the EM insulator centerline, Case 6, is clearly the poorest performer from any of the analysis runs with this projectile.

The EM projectile cases exhibit trends comparable to those found with the M829. Namely, the insulator centerline subjects the round to the most severe angular velocity, while the EM rail profile shows only slightly worse results than the conventional gun case. Also, it is noted how a change in interior ballistic loading results in little difference between the EM and conventional cases. These EM projectile cases have an increasingly higher angular velocity when going from the soft to medium contacts, but the magnitude of the angular rate levels off and does not increase for the stiffest contacts. This is another indication that the medium contact stiffness possibly excites a natural bending frequency of the rod.

In comparing the EM projectile to the M829, it is seen that the EM round has consistently higher angular rates for the soft contact cases. Also, given the conventional gun centerline, both projectiles show angular velocities of equivalent magnitude. Thus, there appears to be nothing inherent in the different projectile designs that causes an aggravation of the in-bore yaw.

9. CONCLUSIONS

From this analysis, it is clear that the EM gun system presents a more severe environment than a conventional powder gun. The results point to the difference in centerlines as a primary cause. Changes in interior ballistic input are shown to have little effect on the transverse acceleration and angular velocity over the length of in-bore travel. However, further studies are required to ascertain if this holds true for velocities well above those of today's ordnance (e.g., 2.5 km/s and higher).

The differences between the M829 and EM projectile geometries do not greatly influence the in-bore yawing motion. In general, the EM projectile is consistently subjected to larger transverse accelerations, but the difference is minimal. Also, the apparent tendency to excite natural frequencies of the

subprojectile for the medium spring stiffness case is certainly something that the EM projectile designer must be concerned with and try to avoid.

The gun barrel centerline profile acts as the principal driver in determining the projectile response for this study. While the rail profile results in yawing motion only slightly worse than the powder gun, the insulator profile clearly brings about the worst response, with both the transverse accelerations and angular velocities being substantially higher.

The one-dimensionality of the RASCAL analysis fails to account for any coupling effects that result from traversing the rail and insulator centerlines simultaneously. Since it has been shown that the rail centerline imparts more motion to the projectile than a conventional gun, and the insulator centerline produces even greater motion, it is believed a more advanced code capable of modeling the full internal bore geometry will show even more deleterious results.

Finally, the results of this analysis point out a weakness of the current EM gun systems, that being an inability to maintain a relatively benign centerline through which the projectile traverses. At present, EM railguns have centerlines that fluctuate from shot to shot. Until a less severe centerline profile can be maintained on a consistent basis, EM projectiles will have difficulty matching the in-bore, and subsequently, the flight, accuracy, and terminal performance of rounds fired from conventional guns.

10. REFERENCES

Erline, T. F. "Projectile Spring Constants: Significance to Modeling With the Little RASCAL Gun Dynamics Program." BRL-TR-3224, U.S. Army Ballistic Research Laboratory, Aberdeen Proving Ground, MD, April 1991.

Erline, T. F., and M. D. Kregel. "Flexible Projectile Modeling Using the Little RASCAL Gun Dynamics Program." Proceedings of the Sixth U.S. Army Symposium on Gun Dynamics, Tamiment, PA, May 1990.

Erline, T. F., M. D. Kregel, and M. Pantano. "Gun and Projectile Flexural Dynamics Modeled by the Little RASCAL—a User's Manual." BRL-TR-3122, U.S. Army Ballistic Research Laboratory, Aberdeen Proving Ground, MD, July 1990.

Hopkins, D. A. "Modeling Gun Dynamics With Three-Dimensional Beam Elements." Proceedings of the Sixth U.S. Army Symposium on Gun Dynamics, Tamiment, PA, May 1990.

Lyon, D. H. "Radial Stiffness Measurements of Several 120-mm Projectiles." Proceedings of the Seventh U.S. Army Symposium on Gun Dynamics, Newport, RI, May 1993.

Manners, N. D. "A Theoretical Study Into the Effect of Sabot Stiffness on Projectile In-Bore Motion and Launch Accuracy." Proceedings of the Sixth U.S. Army Symposium on Gun Dynamics, Tamiment, PA, May 1990.

McCall, C. D., and D. L. Henry. "Flexural Characteristics of the M829 Projectile Family." U.S. Army Research Laboratory, Aberdeen Proving Ground, MD, to be published.

Polcyn, M. A., and P. A. Cox. "The Adaptation of NASTRAN for Three-Dimensional Gun Dynamics Problems." Proceedings of the Sixth U.S. Army Symposium on Gun Dynamics, Tamiment, PA, May 1990.

Rabern, D. A., and K. A. Bannister. "Finite Element Models to Predict the Structural Response of 120-mm Sabot/Rods During Launch." Proceedings of the Sixth U.S. Army Symposium on Gun Dynamics, Tamiment, PA, May 1990.

Wilkerson, S. A. "The Use of Advanced Structural Codes to Study Gun Dynamics." ARL-TR-49, U.S. Army Research Laboratory, Aberdeen Proving Ground, MD, February 1993.

INTENTIONALLY LEFT BLANK.

No. of Copies	Organization
2	Administrator Defense Technical Info Center ATTN: DTIC-DDA Cameron Station Alexandria, VA 22304-6145
1	Commander U.S. Army Materiel Command ATTN: AMCAM 5001 Eisenhower Ave. Alexandria, VA 22333-0001
1	Director U.S. Army Research Laboratory ATTN: AMSRL-OP-CI-AD, Tech Publishing 2800 Powder Mill Rd. Adelphi, MD 20783-1145
1	Director U.S. Army Research Laboratory ATTN: AMSRL-OP-CI-AD, Records Management 2800 Powder Mill Rd. Adelphi, MD 20783-1145
2	Commander U.S. Army Armament Research, Development, and Engineering Center ATTN: SMCAR-IMI-I Picatinny Arsenal, NJ 07806-5000
2	Commander U.S. Army Armament Research, Development, and Engineering Center ATTN: SMCAR-TDC Picatinny Arsenal, NJ 07806-5000
1	Director Benet Weapons Laboratory U.S. Army Armament Research, Development, and Engineering Center ATTN: SMCAR-CCB-TL Watervliet, NY 12189-4050
1	Director U.S. Army Advanced Systems Research and Analysis Office (ATCOM) ATTN: AMSAT-R-NR, M/S 219-1 Ames Research Center Moffett Field, CA 94035-1000

No. of Copies	Organization
1	Commander U.S. Army Missile Command ATTN: AMSMI-RD-CS-R (DOC) Redstone Arsenal, AL 35898-5010
1	Commander U.S. Army Tank-Automotive Command ATTN: AMSTA-JSK (Armor Eng. Br.) Warren, MI 48397-5000
1	Director U.S. Army TRADOC Analysis Command ATTN: ATRC-WSR White Sands Missile Range, NM 88002-5502
(Class. only) 1	Commandant U.S. Army Infantry School ATTN: ATSH-CD (Security Mgr.) Fort Benning, GA 31905-5660
(Unclass. only) 1	Commandant U.S. Army Infantry School ATTN: ATSH-WCB-O Fort Benning, GA 31905-5000
1	WL/MNOI Eglin AFB, FL 32542-5000
	<u>Aberdeen Proving Ground</u>
2	Dir, USAMSAA ATTN: AMXSY-D AMXSY-MP, H. Cohen
1	Cdr, USATECOM ATTN: AMSTE-TC
1	Dir, ERDEC ATTN: SCBRD-RT
1	Cdr, CBDA ATTN: AMSCB-CII
1	Dir, USARL ATTN: AMSRL-SL-I
5	Dir, USARL ATTN: AMSRL-OP-CI-B (Tech Lib)

No. of Copies	Organization
11	Director Benet Weapons Laboratory U.S. Army Armament Research, Development, and Engineering Center ATTN: SMCAR-CCB, F. Heizer J. Keane T. Allen J. Vasilakis G. Friar J. Zweig T. Simkins V. Montvori J. Wrzochalski G. D'Andrea R. Hasenbein Watervliet, NY 12189
1	Commander ATTN: SMCWV-QAE-Q, C. Howd Bldg. 44 Watervliet Arsenal Watervliet, NY 12189-4050
1	Commander ATTN: SMCWV-SPM, T. McCloskey Bldg. 25/3, Watervliet Arsenal Watervliet, NY 12189-4050
9	Commander U.S. Army Armament Research, Development, and Engineering Center ATTN: SMCAR-CCH-T, S. Musalli P. Christian K. Fehsal N. Krasnow R. Carr SMCAR-CCH-V, E. Fennell SMCAR-CCH, J. DeLorenzo SMCAR-CC, J. Hedderich SMCAR-CCH-P, J. Lutz Picatinny Arsenal, NJ 07806-5000
3	Commander U.S. Army Armament Research, Development, and Engineering Center ATTN: SMCAR-TD, R. Price V. Linder T. Davidson Picatinny Arsenal, NJ 07806-5000
1	Commander Production Base Modernization Activity U.S. Army Armament Research, Development, and Engineering Center ATTN: AMSMC-PBM-K Picatinny Arsenal, NJ 07806-5000
1	Commander U.S. Army Belvoir RD&E Center ATTN: STRBE-JBC, C. Kominos Fort Belvoir, VA 22060-5606
2	Commander U.S. Army Missile Command ATTN: AMSMI-RD, W. McCorkle AMSMI-RD-ST, P. Doyle Redstone Arsenal, AL 35898
3	Commander U.S. Army Armament Research, Development, and Engineering Center ATTN: SMCAR-FSA-M, R. Botticelli F. Diorio SMCAR-FSA, C. Spinelli Picatinny Arsenal, NJ 07806-5000
6	Commander U.S. Army Armament Research, Development, and Engineering Center ATTN: SMCAR-FSE, T. Gora E. Andricopoulos B. Knutelsky A. Graf J. Bennett C. Dunham Picatinny Arsenal, NJ 07806-5000

No. of Copies	Organization
3	Project Manager Advanced Field Artillery System ATTN: COL Napoliello LTC A. Ellis G. DelCoco Picatinny Arsenal, NJ 07806-5000
1	Commander Watervliet Arsenal ATTN: SMCWV-QA-QS, K. Insco Watervliet, NY 12189-4050
2	Project Manager SADARM Picatinny Arsenal, NJ 07806-5000
7	Project Manager Tank Main Armament Systems ATTN: SFAE-AR-TMA, COL Hartline C. Kimker SFAE-AR-TMA-MD, H. Yuen J. McGreen SFAE-AR-TMA-MS, R. Joinson D. Guziewicz SFAE-AR-TMA-MP, W. Lang Picatinny Arsenal, NJ 07806-5000
1	U.S. Army Research Laboratory Advanced Concepts and Plans ATTN: AMSRL-CP-CA, D. Snider 2800 Powder Mill Rd. Adelphi, MD 20783
1	U.S. Army Materiel Command ATTN: AMCSCI, R. Chait 5001 Eisenhower Ave. Alexandria, VA 22333-0001
2	PEO-Armaments ATTN: SFAE-AR-PM, D. Adams T. McWilliams Picatinny Arsenal, NJ 07806-5000

No. of Copies	Organization
2	U.S. Army Research Office Dir., Math & Computer Sciences Div. ATTN: A. Crowson AMXRO-MCS, J. Chandra P.O. Box 12211 Research Triangle Park, NC 27709-2211
6	Director U.S. Army Research Laboratory Materials Technology Directorate ATTN: AMSRL-MA-P, L. Johnson B. Halpin T. Chou AMSRL-MA-PA, D. Granville W. Haskell AMSRL-MA-MA, G. Hagnauer Watertown, MA 02172-0001
2	Commander DARPA ATTN: J. Kelly B. Wilcox 3701 North Fairfax Dr. Arlington, VA 22203-1714
2	NASA Langley Research Center Mail Stop 266 ATTN: F. Barlett, Jr. AMSRL-VS, W. Elber Hampton, VA 23681-0001
1	Commander Wright-Patterson Air Force Base ATTN: AFWAML, R. Kim Dayton, OH 45433
1	Naval Research Laboratory Code 6383 ATTN: Dr. I. Wolock Washington, DC 20375-5000
1	Office of Naval Research Mechanical Division Code 1132-SM ATTN: Y. Rajapakse Arlington, VA 22217

No. of Copies	Organization
2	David Taylor Research Center ATTN: R. Rockwell W. Phyillaier Bethesda, MD 20054-5000
1	David Taylor Research Center Ship Structures and Protection Dept. ATTN: J. Corrado, Code 1702 Bethesda, MD 20084
4	Director Lawrence Livermore National Laboratory ATTN: R. Christensen S. deTeresa W. Feng F. Magness P.O. Box 808 Livermore, CA 94550
2	Pacific Northwest Laboratory A Div of Battelle Memorial Inst. Technical Information Section ATTN: M. Smith M. C.C. Bampton P.O. Box 999 Richland, WA 99352
6	Director Sandia National Laboratories Applied Mechanics Department, Division-8241 ATTN: C. Robinson G. Benedetti W. Kawahara K. Perano D. Dawson P. Nielan P.O. Box 969 Livermore, CA 94550-0096
1	Director Los Alamos National Laboratory ATTN: D. Rabern MEE-13, Mail Stop J-576 P.O. Box 1633 Los Alamos, NM 87545
1	The University of Texas at Austin Center for Electromechanics ATTN: J. Price 10100 Burnet Rd. Austin, TX 78758-4497
2	Virginia Polytechnical Institute and State University, Dept. of ESM ATTN: M. W. Hyer K. L. Reifsnider Blacksburg, VA 24061-0219
2	University of Dayton Research Institute ATTN: R. Y. Kim A. K. Roy 300 College Park Ave. Dayton, OH 45469-0168
1	University of Dayton ATTN: J. M. Whitney 300 College Park Ave. Dayton, OH 45469-0240
1	Drexell University ATTN: A. S. D. Wang 32nd and Chestnut Sts. Philadelphia, PA 19104
1	Purdue University School of Aeronautics and Astronautics ATTN: C. T. Sun West Lafayette, IN 47907-1282
1	University of Kentucky ATTN: L. Penn 763 Anderson Hall Lexington, KY 40506-0046
3	University of Delaware Center for Composite Materials ATTN: J. Gillespe B. Pipes M. Santare 201 Spencer Laboratory Newark, DE 19716

No. of Copies	Organization
2	North Carolina State University Civil Engineering Department ATTN: W. Rasdorf L. Spainhour P.O. Box 7908 Raleigh, NC 27696-7908
1	University of Utah Dept. of Mechanical and Industrial Engineering ATTN: S. Swanson Salt Lake City, UT 84112
1	Stanford University Dept. of Aeronautics and Aeroballistics Durant Building ATTN: S. Tsai Stanford, CA 94305
1	Pennsylvania State University ATTN: R. S. Engle 245 Hammond Bldg. University Park, PA 16801
1	Pennsylvania State University ATTN: D. W. Jensen 223-N Hammond University Park, PA 16802
1	Pennsylvania State University ATTN: R. McNitt 227 Hammond Building University Park, PA 16802
1	UCLA MANE Department, Engineering IV ATTN: H. T. Hahn Los Angeles, CA 90024-1597
1	University of Illinois at Urbana-Champaign National Center for Composite Materials Research 216 Talbot Laboratory ATTN: J. Economy 104 S. Wright St. Urbana, IL 61801

No. of Copies	Organization
1	IAP Research, Inc. ATTN: A. Challita 2763 Culver Ave. Dayton, OH 45429
2	Olin Corporation Flinchbaugh Division ATTN: E. Steiner B. Stewart P.O. Box 127 Red Lion, PA 17356
1	Olin Corporation ATTN: L. Whitmore 10101 9th St., North St. Petersburg, FL 33702
3	Alliant Techsystems, Inc. ATTN: C. Candland J. Bode K. Ward 5901 Lincoln Dr. Minneapolis, MN 55346-1674
1	Alliant Techsystems, Inc. Precision Armaments Systems Group 7225 Northland Dr. Brooklyn Park, MN 55428
1	Chamberlain Manufacturing Corporation Research and Development Division ATTN: T. Lynch 550 Esther St. P.O. Box 2335 Waterloo, IA 50704
1	Custom Analytical Engineering Systems, Inc. ATTN: A. Alexander Star Route, Box 4A Flintstone, MD 21530
2	Institute for Advanced Technology ATTN: T. Kiehne H. Fair 4030-2 W. Braker La. Austin, TX 78759

No. of Copies	Organization
2	Kaman Sciences Corporation ATTN: D. Elder T. Hayden P.O. Box 7463 Colorado Springs, CO 80933
3	LORAL/Vought Systems ATTN: G. Jackson K. Cook L. L. Hadden 1701 W. Marshall Dr. Grand Prairie, TX 75051
1	Interferometrics, Inc. ATTN: R. Larriva, Vice President 8150 Leesburg Pike Vienna, VA 22100
1	ARMTEC Defense Products ATTN: S. Dyer 85-901 Ave. 53 P.O. Box 848 Coachella, CA 92236
	Aberdeen Proving Ground
12	Dir, USARL ATTN: AMSRL-SL-BE, Chief AMSRL-WT-WC, Chief AMSRL-WT-WB, W. D'Amico A. Zielinski J. Powell AMSRL-WT-TC, W. de Rosset R. Coates AMSRL-WT-TA, W. Gillich AMSRL-WT-PE, Chief AMSRL-WT-PA, Chief AMSRL-WT-PC, Chief AMSRL-WT-PB, Chief

No. of Copies	Organization
	Aberdeen Proving Ground (continued)
14	AMSRL-WT-PD, R. Burns T. Bogetti J. Bender J. Ford R. Murray R. Kirkendall T. Erline D. Hopkins S. Wilkerson R. Kaste L. Burton J. Tzeng W. Drysdale K. Bannister
	Adelphi
9	Dir, USARL ATTN: AMSRL-WT-PD (ALC), A. Abrahamian K. Barnes M. Berman H. Davison A. Frydman T. Li W. McIntosh E. Szymanski H. Watkins

This Laboratory undertakes a continuing effort to improve the quality of the reports it publishes. Your comments/answers to the items/questions below will aid us in our efforts.

1. ARL Report Number ARL-TR-295 Date of Report October 1993

2. Date Report Received ____________________

3. Does this report satisfy a need? (Comment on purpose, related project, or other area of interest for which the report will be used.) ____________________

4. Specifically, how is the report being used? (Information source, design data, procedure, source of ideas, etc.) ____________________

5. Has the information in this report led to any quantitative savings as far as man-hours or dollars saved, operating costs avoided, or efficiencies achieved, etc? If so, please elaborate. ____________________

6. General Comments. What do you think should be changed to improve future reports? (Indicate changes to organization, technical content, format, etc.) ____________________

CURRENT ADDRESS

Organization

Name

Street or P.O. Box No.

City, State, Zip Code

7. If indicating a Change of Address or Address Correction, please provide the Current or Correct address above and the Old or Incorrect address below.

OLD ADDRESS

Organization

Name

Street or P.O. Box No.

City, State, Zip Code

(Remove this sheet, fold as indicated, tape closed, and mail.)
(DO NOT STAPLE)

DEPARTMENT OF THE ARMY

OFFICIAL BUSINESS

NO POSTAGE
NECESSARY
IF MAILED
IN THE
UNITED STATES

BUSINESS REPLY MAIL

FIRST CLASS PERMIT No 0001, APG, MD

Postage will be paid by addressee.

Director
U.S. Army Research Laboratory
ATTN: AMSRL-OP-CI-B (Tech Lib)
Aberdeen Proving Ground, MD 21005-5066